Occurrence of kornerupine-bearing granulite from Karimnagar, Andhra Pradesh

I. N. Sharma and D. Prakash*

Department of Geology, Banaras Hindu University, Varanasi 221 005, India

Here, we report the occurrence of kornerupine–bearing, quartz-free granulite from the Malial area of Karimnagar district, Andhra Pradesh. It occurs as small enclaves and pods within the granite-gneiss, associated with garnet–orthopyroxene–cordierite–biotite-gneiss. Its mineral assemblage includes kornerupine–cordierite–biotite–spinel, K-feldspar, ilmenite and magnetite. Kornerupine, a hydrated magnesium–aluminium silicate plots on the $4MgO–3Al_2O_3–4SiO_2$ (4 : 3 : 4) composition along the solid solution join between 4 : 3 : 4 and 1 : 1 : 1 ($3.5MgO.3.5Al_2O_3.3.5SiO_2$) compositions. The relative X_{Mg} values among various minerals are as follows: cordierite > biotite > kornerupine > spinel. The deduced post-peak metamorphic pressure–temperature conditions of 5–6 kbar and 650–750°C for the kornerupine–spinel–bearing quartz-free granulites are consistent with the experimental work on stability of kornerupine in the $MgO–Al_2O_3–SiO_2–H_2O$ system.

Keywords: Andhra Pradesh, granulite, kornerupine, MASH system, *P–T* estimate.

KORNERUPINE is a rare mineral in metamorphic terrains and has been reported from a few localities only in India. The first report of kornerupine in India was made by Murthy[1] from Rannu, Uttar Pradesh. Later Balasubrahmanyan[2] and Lal *et al.*[3] reported kornerupine in a sapphirine-bearing granulite from Kovilpatti, Madras and Sonapahar, Assam respectively. Grew[4] has described five localities of kornerupine-bearing granulites from the Southern Granulite belt and the Eastern Ghats belt. Recently Sajeev *et al.*[5] reported kornerupine from the Ganguvarpatti, South India. In the Karimnagar area, kornerupine occurs as large prograde porphyroblasts in rocks devoid of sapphirine, whereas it is associated with sapphirine as prismatic aggregates in the above-mentioned areas, except Kondapalle. Kornerupine-bearing granulites have been reported from seventy other Precambrian regional terrains of the world, including Germany[6,7], Greenland[8], Australia[9,10], South Africa[11], Sri Lanka[12] and East Antarctica[13].

Earlier sapphirine–spinel-bearing rocks from the Eastern Dharwar Craton (EDC) in the Karimnagar area were reported by Sarvothaman[14]. Karimnagar and its adjoining areas have attracted attention of petrologists on account of the increasingly useful high-grade rocks that serve as a window for the mid-lower continental crust.

*For correspondence. (e-mail: dprakash_ynu@yahoo.com)

Quartz-free kornerupine-bearing granulite has been found nearly 2 km SE of Malial village in Karimnagar district, Andhra Pradesh (78°58′30″E long. and 18°41′30″N lat. in the Survey of India toposheet 56J/14; Figure 1).

Karimnagar area is predominantly a granite-gneiss terrain along with exposures of charnockite, banded magnetite, quartzite and dolerite dykes. The granite-gneisses and charnockites contain enclaves of high-grade supracrustals, including quartz-free sapphirine–spinel granulites, gneisses and basic granulites, which rarely occur in the entire northeastern portion of EDC. Varieties of rocks from the study area reveal a wide range of mineral parageneses and chemical compositions[15]. The major rock types include charnockites (Opx–Pl–Perth–Qtz ± Bt ± Grt), gneisses (Opx–Crd–Bt–Pl–Qtz–Perth ± Grt ± Sil ± Spl; Bt–Qtz–Pl ± Crd ± Hbl ± Spl), basic granulites (Cpx–Pl–Qtz ± Opx ± Hbl), quartz-free granulites (Spr–Spl–Crd–Bt ± Opx ± Kfs, Bt–Crd–Krn–Spl ± Kfs, And–Bt–Kfs–Chl), granites (Qtz–Pl–Kfs ± Bt ± Hbl), meta-dolerites (Cpx–

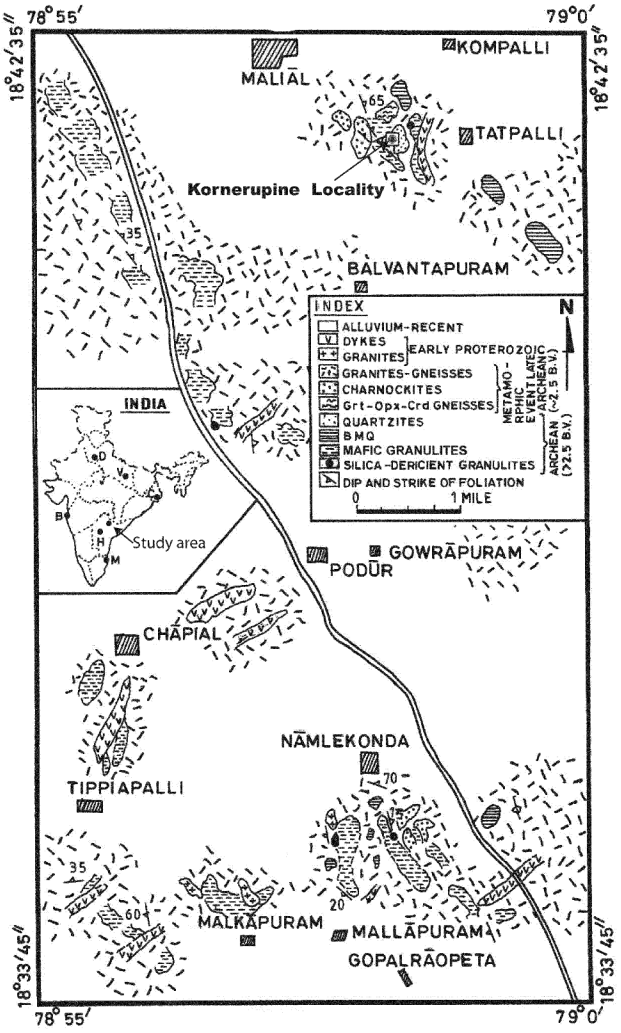

Figure 1. Geological map of the area NW of Karimnagar.

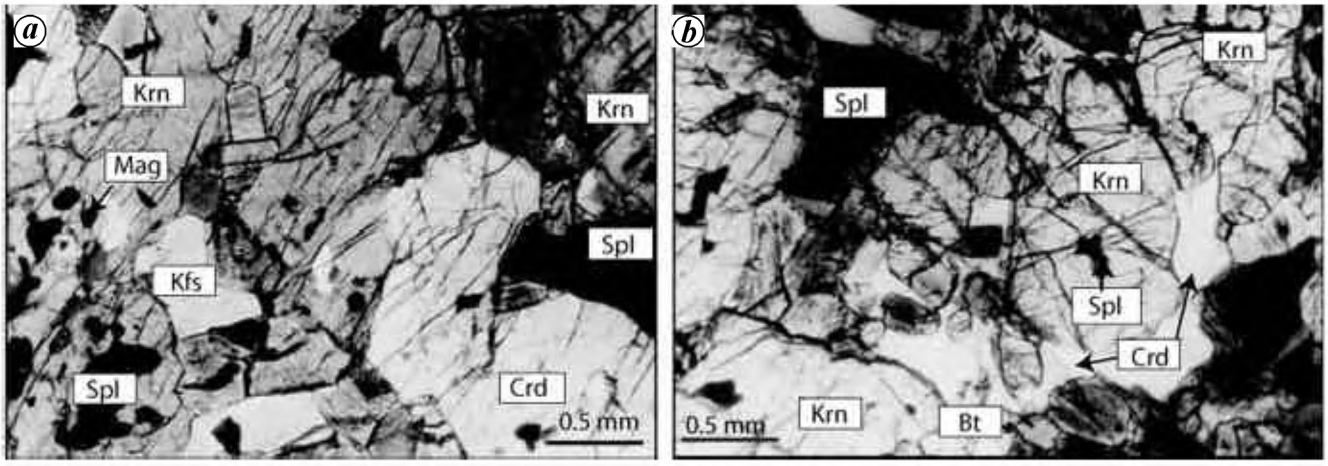

Figure 2. ***a***, Photomicrograph of kornerupine-bearing quartz-free granulite showing fractured megacryst of kornerupine having prominent inclusion of spinel. Cordierite is present in the matrix (under crossed nicols). ***b***, Photomicrograph showing spinel and cordierite isolated to form coarse idioblastic or subidioblastic kornerupine (under plane polarized light). Krn, Kornerupine; Crd, Cordierite; Spl, Spinel; Bt, Biotite; Kfs, Potash feldspar; Mag, Magnetite.

Pl ± Bt ± Qtz ± Chl), banded magnetite quartzites and quartzites.

Rajesham *et al.*[16] dated the charnockites and granite-gneisses from the Karimnagar area having Rb–Sr isochron age of ~2500 Ma and interpreted it to represent single major metamorphic event; the high-grade supracrustals that occur as enclaves in these should be obviously older than 2500 Ma.

Kornerupine-bearing rock is dark coloured, massive and coarse-grained. It shows inequigranular granoblastic texture (Figure 2 *a*). The main assemblage includes kornerupine–cordierite–biotite–spinel ± potash feldspar ± ilmenite, magnetite (minor amount).

Kornerupine is colourless, feebly pleochroic and occurs as coarse prismatic crystals. Spinel and cordierite are isolated to form coarse idioblastic or subidioblastic kornerupine (Figure 2 *b*) that marks the following reaction:

Spinel + cordierite + vapour = kornerupine ± corundum.

Biotite flakes are present as inclusions and also in direct grain contact with kornerupine. Idioblastic to subidioblastic grains of spinel are also found as inclusions within kornerupine and nowhere in direct contact with cordierite and biotite. Potash feldspar is present in minor amount. Thin sections do not preserve complete reaction textures like coronas and symplectites to infer any other reaction.

Representative electron microprobe data of kornerupine and associated minerals are given in Table 1. Electron microprobe analysis was carried out in the EPMA Laboratory, IIT Roorkee on a JEOL JXA-8600M unit with three fully focused spectrometers. Carbon-coated thin sections of approximately 40 μm thickness were used for analysis. The instrument was operated at a probe current of 2×10^{-8} A with an accelerating voltage of 15 kV and electron beam diameter of 2 μm. ZAF oxide correction was made.

Kornerupine is a hydrated magnesium–aluminium silicate and the analyses plot on the $4MgO.3Al_2O_3.4SiO_2$ (4 : 3 : 4) composition (Figure 3) along the solid solution join between 4 : 3 : 4 and 1 : 1 : 1 ($3.5MgO.3.5Al_2O_3.3.5SiO_2$) with slight deficiency in Si, Mg and higher Al. Appreciable amount of Fe^{3+} is present ranging between 0.128 and 0.139 p.f.u. X_{Mg} [$X_{Mg} = Mg/(Mg + Fe^{2+})$] values show a restricted range between 0.786 and 0.795. Boron was not sought. The name prismatine[6,17] has been recently revalidated for kornerupine having boron > 0.5 p.f.u. Cordierite is the most magnesian phase (X_{Mg}: 0.851). Biotite has X_{Mg} ranging between 0.814 and 0.849, with low fluorine content. Spinel (hercynite) is relatively iron-rich (X_{Mg}: 0.382) in kornerupine-bearing rocks compared to other quartz-free granulites. The relative X_{Mg} variation in the different phases is cordierite > biotite > kornerupine > spinel (I. N. Sharma, unpublished).

Kornerupine and other minerals from the quartz-free granulites have been plotted in the SiO_2–(Mg, Fe)O–(Al, Fe^{3+}, Cr)$_2O_3$ triangular diagram (Figure 4 *a*). The important mineral phase, biotite does not plot in this diagram and has to be treated as an excess phase. To resolve this problem, a projection from potash feldspar (Figure 4 *b*) has been used in the triangular diagram $\{SiO_2–6(K_2O + Na_2O)\}$ – (Fe, Mg)O – $\{(Al, Cr, Fe^{3+})_2O_3 – (K_2O + Na_2O)\}$.

Kornerupine-bearing quartz-free granulites are found in association of gneisses and two-pyroxene granulites. The gneisses contain garnet, orthopyroxene, cordierite, biotite and feldspar as the main minerals, whereas two-pyroxene granulites consist of orthopyroxene, clinopyroxene, hornblende and plagioclase as the major minerals.

Precise geothermobarometric estimates have not been made for the kornerupine-bearing quartz-free granulites due to lack of well-defined thermodynamic data for kornerupine and absence of relevant phases as *P–T* sensors. However, a reasonable *P–T* estimate on the basis of conventional

Table 1. Representative microprobe analyses of the coexisting minerals (sample no. 69XIX)

	Krn		Crd	Bt		Spl
Spot no.	1R	2R	3C	4R	5R	6C
SiO_2	29.73	29.24	49.82	37.39	38.96	0.00
TiO_2	0.06	0.04	0.00	1.07	2.62	0.02
Al_2O_3	41.01	40.98	32.56	16.49	15.57	57.99
Cr_2O_3	0.20	0.13	n.d.	0.06	0.12	3.14
FeO**	8.53	8.75	3.58	7.21	8.55	28.87
MnO	0.19	0.29	0.04	0.00	0.00	0.15
MgO	15.68	15.10	11.54	22.73	21.04	9.24
ZnO	n.d.	n.d.	n.d.	0.00	0.00	0.54
CaO	0.03	0.02	0.03	0.05	0.00	0.00
Na_2O	0.03	0.06	0.08	0.18	0.13	n.d.
K_2O	n.d.	n.d.	0.00	8.71	8.58	n.d.
F	n.d.	n.d.	n.d.	0.07	0.10	n.d.
–O	–	–	–	0.03	0.04	–
Total	95.46	94.61	97.63	93.93	95.63	100.35
Oxygen basis	21	21	18	22	22	8
Si	3.821	3.798	5.053	5.433	5.569	0.000
Al^{IV}	0.179	0.202	3.889*	2.567	2.431	3.748*
Al^{VI}	6.035	6.073	–	0.263	0.198	–
Ti	0.006	0.004	0.000	0.114	0.284	0.001
Cr	0.020	0.014	n.d.	0.007	0.014	0.138
Fe^{3+}	0.128	0.139	n.d.	n.d.	n.d.	0.110
Fe^{2+}	0.774	0.796	0.305	0.873	1.023	1.221
Mn	0.021	0.032	0.004	0.000	0.000	0.007
Mg	3.004	2.923	1.743	4.926	4.486	0.754
Zn	n.d.	n.d.	n.d.	0.000	0.000	0.022
Ca	0.004	0.003	0.003	0.008	0.000	0.000
Na	0.008	0.016	0.012	0.050	0.036	n.d.
K	n.d.	n.d.	0.000	1.608	1.564	n.d.
F	n.d.	n.d.	n.d.	0.032	0.046	n.d.
X_{Mg}	0.795	0.786	0.851	0.849	0.814	0.382

n.d., Not determined; C, Core; R, Rim; *, Total Al in place of Al^{IV} and Al^{VI}; **, Total iron as FeO, $Fe^{3+} = 42 - [(2R^{2+}) + (3R^{3+}) + (4R^{4+})]$ for kornerupine and $Fe^{3+} = 16 - [(2R^{2+}) + (3R^{3+}) + (4R^{4+})]$ for spinel.

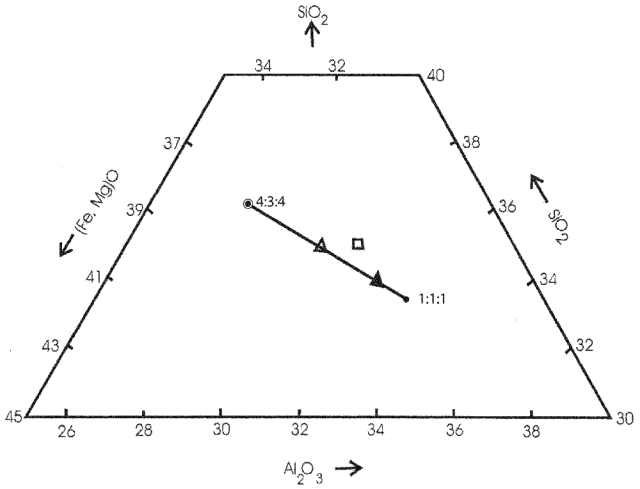

Figure 3. $(Fe^{2+}, Mg)O–Al_2O_3–SiO_2$ triangular plot showing kornerupine composition. Open circle indicates composition of kornerupine from the study area. Open triangle (Ellammankovilpatti), square (Ganguvarpatti) and solid triangle (Ponakkadu) are kornerupine composition plots from Grew[4] for comparison purpose.

geothermobarometry and convergence method for the retrieval of peak *P–T* conditions applicable to the associated rocks has been attempted. Basic granulites yield a value of 7–8 kbar and 800–850°C. The average temperature (600–750°C) for the adjoining garnet–orthopyroxene–cordierite–biotite-gneiss is obtained from various Fe^{2+}–Mg exchange models of garnet–biotite, garnet–cordierite and garnet–orthopyroxene pairs. Lower values from the garnet–biotite Fe^{2+}–Mg exchange geothermometers may be due to re-equilibration during retrogression. Average pressure in the range of 4.5–6 kbar at 700°C is obtained by various geobarometric models of garnet–cordierite–sillimanite–quartz and garnet–orthopyroxene–plagioclase–quartz applied to the garnet–orthopyroxe–cordierite–biotite–gneiss (Table 2).

According to Seifert[18], boron-free kornerupine has been synthesized in the system $MgO–Al_2O_3–SiO_2–H_2O$ (MASH) at water pressure above 4.5 kbar and temperatures in excess of 735°C. Syntheses of boron-free kornerupine have also been described by Schreyer and Seifert[19], and

Table 2. *P–T* estimate for Grt–Opx–Crd–Bt-gneiss (sample 508a)

Sample 508a/spot no.	$(X_{Mg})^{Grt}$	$(X_{Mg})^{Bt}$	$(X_{Mg})^{Crd}$	$(X_{Mg})^{Opx}$	$(X_{Ca})^{Pl}$
R6, R3 (Grt–Bt)	0.277	0.727	–	–	–
R28, R9 (Grt–Crd)	0.256	–	0.748	–	–
C13, C9, C3 (Grt–Opx–Pl)	0.321	–	–	0.618	0.416

Temperature (°C) at 6 kbar				Pressure (kbar) at 700°C			
	Grt–Bt	Grt–Crd	Grt–Opx	Grt–Crd–Sil–Qtz		Grt–Opx–Pl–Qtz	
K_d	5.577	8.000	2.774	P_{Mg}	P_{Fe}	P_{Mg}	P_{Fe}
ln K_d	1.719	2.079	1.020				
1.	605	674	778	6.01	6.38	–	4.82
2.	585	722	713	6.02	–	–	4.43
3.	647	683	735	–	5.30	4.02	3.51
4.	584	666	669	6.23	–	4.10	4.30
5.	596	623	698	4.80	5.40	4.25	4.27
Average	603 ± 26	674 ± 36	719 ± 41	5.77 ± 0.65	5.69 ± 0.60	4.12 ± 0.12	4.27 ± 0.48

Grt–Bt: 1. Thompson[24]; 2. Ferry and Spear[23]; 3. Dasgupta *et al.*[27]; 4. Bhattacharya *et al.*[27] (Hackler and Wood[28]); 5. Berman[29] (with ideal biotite).
Grt–Crd: 1. Thompson[24]; 2. Bhattacharya *et al.*[30]; 3. Aranovich and Podlesskii[31]; 4. Perchuk[32]; 5. Nichols *et al.*[33].
Grt–Opx: 1. Sen and Bhattacharya[34]; 2. Harley[35]; 3. Bhattacharya *et al.*[27]; 4. Berman[29], 5. Lal[36].
Grt–Crd–Sil–Qtz: 1. Thompson[24]; 2. Perchuk *et al.*[37]; 3. Bhattacharya[38]; 4. Aranovich and Podlesskii[31]; 5. Berman[29].
Grt–Opx–Pl–Qtz: 1. Bohlen *et al.*[39]; 2. Perkins and Chipera[40]; 3. Bhattacharya *et al.*[41]; 4. Berman[29]; 5. Lal[36].

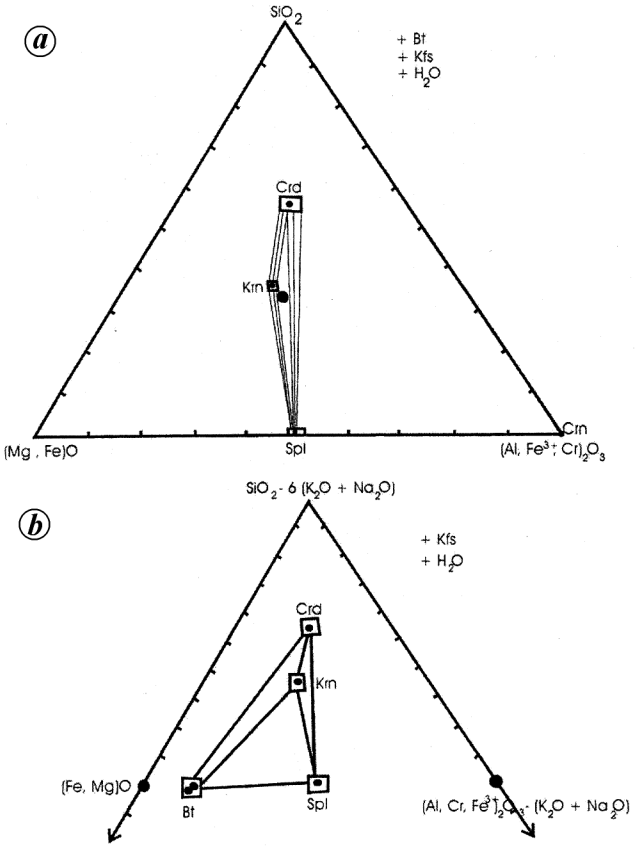

Figure 4. ***a***, Topology of phase relations for quartz-free granulites shown in the SiO_2–(Mg, Fe)O–(Al, Fe^{3+}, Cr)$_2O_3$ triangular diagram. Small solid circles show plot of mineral compositions and large solid circles represent observed mineral parageneses. ***b***, Topological configuration for kornerupine-bearing quartz-free granulites shown in the [(SiO_2–6(K_2O + Na_2O)]–(Fe, Mg)O–[(Al, Cr, Fe^{3+})$_2O_3$–(K_2O + Na_2O)] projection from potash feldspar. Small solid circles show plot of mineral compositions.

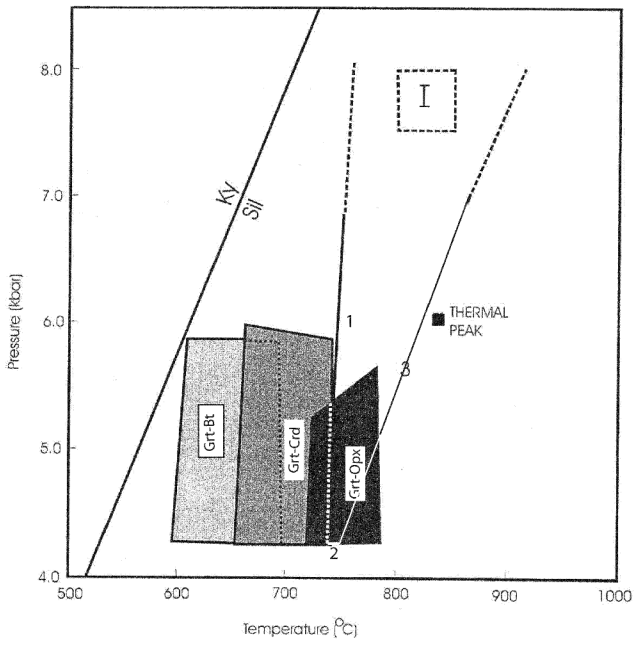

Figure 5. Comparison of stability field of boron-free kornerupine (marked as reactions 1–3) in the kyanite–sillimanite phase diagram along with *P–T* estimates for different high-grade rocks from the study area. (i) Chl + Crd + Crn == Krn + V (lower temperature limit). (ii) Chl + Crd + Spr == Krn ± V (lower pressure limit). (iii) Krn == Crd + En + Spr + V (upper temperature limit). I, *P–T* conditions for basic granulite.

Yoder[20,21]. In the MASH system at pressures in the vicinity of 10 kbar and temperatures around 850°C. Robbins and Yoder[22] have experimentally found that boron-bearing kornerupine is a high temperature breakdown product of tourmaline (dravite) at 895°C and 5 kbar pressure.

The thermal peak of metamorphism (~ 850°C) at moderately high pressures of 6 kbar is more than the upper stability limit of kornerupine (Figure 5). This proves that kornerupine was formed after the thermal peak of metamorphism. *P–T* estimates (700–750°C and 4.5–5.5 kbar) for the associated rocks from the study area lie close to the lower temperature stability field of kornerupine (Figure 5). The presence of iron and lower activity of water may shift the stability field of kornerupine towards the lower temperature side in the $FeO–MgO–Al_2O_3–SiO_2–H_2O$ system.

The absence of anhydrous minerals of granulite facies conditions (orthopyroxene, sapphirine) suggests that kornerupine was formed slightly after the thermal peak conditions of metamorphism during which the activity of water increased, thus providing conditions for the formation of hydrous phases. This observation can further be reinforced by the coarse grain size of kornerupine and its association with other hydrous minerals such as biotite and cordierite, which suggests an increase in the activity of fluids shortly following the metamorphic climax. The estimation of thermal peak of metamorphism at ~ 850°C also reinforces the observation that kornerupine was formed after the metamorphic peak. The only mineral remnant of the thermal peak is spinel. This type of late post-metamorphic mineral generation due to the influence of fluids from crystallizing partial melts has been reported from Broken Hill, Australia[23].

1. Murthy, M. V. N., Kornerupine from Rannu, Uttar Pradesh. *Nature*, 1954, **174**, 1065.
2. Balasubrahmanyan, M. N., Note on kornerupine from Ellammankovilpatti, Madras. *Mineral. Mag.*, 1965, **35**, 662–664.
3. Lal, R. K., Ackermand, D., Seifert, F. and Haldar, S. K., Chemographic relationships in sapphirine-bearing rocks from Sonapahar, Assam, India. *Contrib. Mineral. Petrol.*, 1978, **67**, 169–187.
4. Grew, E. S., Sapphirine, kornerupine and sillimanite + orthopyroxene in the charnockitic region of South India. *J. Geol. Soc. India*, 1982, **23**, 469–505.
5. Sajeev, K., Osanai, Y. and Santosh, M., Ultrahigh-temperature metamorphism followed by two-stage decompression of garnet–orthopyroxene–sillimanite granulites from Ganguvarpatti, Madurai block, southern India. *Contrib. Mineral. Petrol.*, 2004, **148**, 29–46.
6. Rotzler, J., Werner, C.-D. and Kroner, U., *P–T*-time paths, deformation history, and protoliths at the type locality of the granulite. In Excursion Guide for the 11th International Conference on Basement Tectonics (eds Bankwitz, P. and Frischbutter, A.), GeoForschungsZentrum and International Basement Tectonics Association, Potsdam, July 1994, pp. 9–52.
7. Grew, E. S., Borosilicates (exclusive of tourmaline) and boron in rock-forming minerals in metamorphic environments. In *Boron Mineralogy, Petrology and Geochemistry* (eds Grew, E. S. and Anovitz, L. M.), Mineral Soc. Am. Rev. Mineral., 1996, vol. 33, pp. 387–502.
8. Friend, C. R. L., Al–Cr substitution in peraluminous sapphirine from the Bjoncrsund area, Fiskenacsset region, Southern West Greenland. *Mineral. Mag.*, 1982, **46**, 323–328.
9. Goscombe, B., Silica-undersaturated sapphirine, spinel and kornerupine granulite facies rocks, NE Strangways Range, Central Australia. *J. Met. Geol.*, 1992, **10**, 181–201.
10. Vry, J. K. and Cartwright, I., Sapphirine–kornerupine rocks from the Reynolds Range, Central Australia: constraints on the uplift history of a Proterozoic low pressure terrain. *Contrib. Mineral. Petrol.*, 1994, **116**, 78–91.
11. Windley, B. F., Ackermand, D. and Herd, R. K., Sapphirine/kornerupine-bearing rocks and crustal uplift history of the Limpopo belt, Southern Africa. *Contrib. Mineral. Petrol.*, 1984, **86**, 342–358.
12. Sajeev, K. and Osanai, Y., Ultrahigh-temperature metamorphism (150°C, 12 kbar) and multistage evolution of Mg-, Al-rich granulites form the Central Highland Complex, Sri Lanka. *J. Petrol.*, 2004, **45**, 1821–1844.
13. Kelly, N. M. and Harley, S. L., Orthopyroxene-corundum in Mg–Al-rich granulites from the Oygarden Islands, East Antarctica. *J. Petrol.*, 2004, **45**, 1481–1512.
14. Sarvothaman, H., Occurrences of sapphirine-bearing rocks near Jagtiyal, Karimnagar Districtk, AP. *Q. J. Geol. Min. Metall. Soc. India*, 1984, **56**, 202–207.
15. Sharma, I. N., Lal, R. K. and Mohan, A., Chemographic relationship and metamorphic evolution of orthopyroxene or sillimanite-bearing garnet–cordierite-gneisses and sapphirine–spinel–corundum granulites from Karimnagar, NE part of the Eastern Dharwar Craton, India. *Geol. Soc. India Mem.*, 2003, **52**, 195–228.
16. Rajesham, T., Bhaskara Rao, Y. J. and Murti, K. S., The Karimnagar granulite terrane – a new sapphirine-bearing granulite province, South India. *J. Geol. Soc. India*, 1993, **41**, 51–59.
17. Grew, E. S., Cooper, M. A. and Howthorne, F. C., Prismatine: Revalidation for boron-rich compositions in the kornerupine group. *Mineral. Mag.*, 1996, **60**, 483–491.
18. Seifert, F., Boron-free kornerupine: A high-pressure phase. *Am. J. Sci.*, 1975, **275**, 57–87.
19. Schreyer, W. and Seifert, F., High-pressure phases in the system $MgO–Al_2O_3–SiO_2–H_2O$. *Am. J. Sci. A*, 1969, **267**, 407–443.
20. Yoder Jr., H. S., The join diopside–pyrope–H_2O at 10 kb: Its bearing on the melting of peridotite, the ACF metamorphic facies, and the gedrite–hornblende miscibility gap. *Carnegie Inst. Washington Publ.*, 1971, **69**, 176–181.
21. Yoder Jr., H. S., Aluminous anthophyllite: The $MgO–Al_2O_3–SiO_2–H_2O$ system at 850°C and 10 kb. *Carnegie Inst. Washington Publ.*, 1971, **70**, 142–145.
22. Robbins, C. R. and Yoder Jr., H. S., Stability relations of dravite, a tourmaline. *Carnegie Inst. Washington Publ.*, 1962, **61**, 106–107.
23. Corbett, G. J. and Phillips, G. N., Regional retrograde metamorphism of a high-grade terrane: the Willyama Complex, Broken Hill, Australia. *Lithos*, 1981, **14**, 59–73.
24. Thompson, A. B., Mineral reaction in politic rocks: I. Prediction in *P–T–X* (Fe–Mg) phase relations. II. Calculations of some *P–T–X* (Fe–Mg) phase relations. *Am. J. Sci.*, 1976, **276**, 401–454.
25. Ferry, J. M. and Spear, F. S., Experimental calibration of the partitioning of Fe and Mg between biotite and garnet. *Contrib. Mineral. Petrol.*, 1978, **66**, 113–117.
26. Dasgupta, S., Sengupta, P., Guha, D. and Fukuoka, M., A refined garnet–biotite Fe–Mg exchange geothermometer and its application in amphibolites and granulites. *Contrib. Mineral. Petrol.*, 1991, **109**, 130–137.
27. Bhattacharya, A., Mohanty, L., Maji, A., Sen, S. K. and Raith, M., Non-ideal mixing in the phlogopite–annite binary solution: Constraints from experimental data on Mg–Fe partitioning and a reformulation of the biotite–garnet geothermometers. *Contrib. Mineral. Petrol.*, 1992, **111**, 87–93.
28. Hackler, R. T. and Wood, B. J., Experimental determination of Fe and Mg exchange between garnet and olivine and estimation of Fe–Mg garnet mixing properties. *Am. Mineral.*, 1989, **74**, 949–999.
29. Berman, R. G., Internally consistent thermodynamic data for stoichiometric minerals in the system $Na_2O–K_2O–CaO–FeO–Fe_2O_3–Al_2O_3–SiO_2–TiO_2–H_2O–CO_2$. *J. Petrol.*, 1988, **29**, 445–522.

30. Bhattacharya, A., Mazumdar, A. C. and Sen, S. K., Fe–Mg mixing in cordierite: constraints from natural data and implication for cordierite–garnet geothermometry to granulite. *Am. Mineral.*, 1988, **73**, 338–344.
31. Aranovich, L. Y. and Podlesskii, K. K., Geothermobarometry of high-grade metapelites: Simultaneously operating relations. In *Evolution of Metamorphic Belts* (eds Daly, J. S., Cliff, R. A. and Yardley, B. W. D.), Geol. Soc. Spec. Publ., 1989, vol. 43, pp. 45–61.
32. Perchuk, L. L., Derivation of a thermodynamically consistent set of geothermometers and geobarometrs for metamorphic and magmatic rocks. In *Progress in Metamorphic and Magmatic Petrology (A Memorial Volume in Honour of D. S. Korzhinsky)* (ed. Perchuk, L. L.), Cambridge Univ. Press, 1991, pp. 93–111.
33. Nichols, G. T., Berry, R. F. and Green, D. H., Internally consistent gahnitic spinel–cordierite–garnet equilibria in the FMASHZn system; geothermobarometry and application. *Contrib. Mineral. Petrol.*, 1992, **111**, 362–377.
34. Sen, S. K. and Bhattacharya, A., An Opx–Gt geothermometer and its application to the Madras charnockite. *Contrib. Mineral. Petrol.*, 1984, **88**, 64–71.
35. Harley, S. L., An experimental study of the partitioning of Fe and Mg between garnet and orthopyroxene. *Contrib. Mineral. Petrol.*, 1984, **86**, 359–373.
36. Lal, R. K., Internally consistent recalibrations of mineral equilibria for geothermobarometry involving garnet–orthopyroxene–plagioclase–quartz assemblages and their application to the South Indian granulites. *J. Met. Geol.*, 1993, **11**, 855–866.
37. Perchuk, L. L. *et al.*, Precambrian granulites of the Aidam Shield, eastern Siberia. USSR. *J. Met. Geol.*, 1985, **3**, 265–310.
38. Bhattacharya, A., Some geobarometers involving cordierite in the $FeO–Al_2O_3–SiO_2$ ($\pm H_2O$) system: refinements, thermodynamic calibration and applicability in granulite facies rocks. *Contrib. Mineral. Petrol.*, 1986, **98**, 387–394.
39. Bohlen, S. R., Wall, V. J. and Boettcher, A. L., Experimental investigation and application of garnet–granulite equilibria. *Contrib. Mineral. Petrol.*, 1983, **83**, 52–81.
40. Perkins, D. and Chipera, S. J., Garnet–orthopyroxene–plagioclase–quartz barometry: refinement and application to the English river subprovince and the Minnesota River Valley. *Contrib. Mineral. Petrol.*, 1985, **89**, 69–80.
41. Bhattacharya, A., Krishnakumar, K. R., Raith, M. and Sen, S. K., An improved set of *a–x* parameter for Fe–Mg–Ca garnet and refinement of the opx–gt thermometer and the opx–gt–plagioclase–qtz barometer. *J. Petrol.*, 1991, **32**, 629–656.

ACKNOWLEDGEMENTS. This work was supported by a grant from DST, New Delhi to D.P. and a CSIR, RA grant to I.N.S. Help rendered by Dr Manickwasagam and Dr T. Ghosh, USIC, IIT Roorkee during microprobe analyses is acknowledged. We thank Prof. R. K. Lal and Prof. A. Mohan for useful discussions, and Prof. Grew for his comments. The anonymous reviewers are thanked for their constructive comments that led to substantial improvement in the manuscript.

Received 30 January 2006; revised accepted 29 April 2006

Generation of very high resolution gravity image over the Central Indian Ridge and its tectonic implications

T. J. Majumdar*, R. Bhattacharyya and S. Chatterjee

Earth Sciences and Hydrology Division, Marine and Water Resources Group, Remote Sensing Applications and Image Processing Area, Space Applications Centre (ISRO), Ahmedabad 380 015, India

Satellite altimetry can be used to infer subsurface geological structures analogous to gravity anomaly maps generated through ship-borne survey. In this study, free-air gravity image has been generated over the Central Indian Ridge using very high resolution database as obtained from Geosat GM, ERS-1, Seasat and TOPEX/POSEIDON altimeter data. Isostatically compensated regions could be identified with all fracture zones clearly demarcated in this map.

Keywords: Central Indian Ridge, free-air gravity, Geosat geodetic mission, satellite altimetry, seafloor spreading.

THE segment of the northern branch of the mid-Indian Ocean ridge system, which lies between Rodriguez Triple Junction and the equator, broadly forming a north–south lineation, is referred as the Central Indian Ridge (CIR)[1] (Figure 1). The Indian Ocean has experienced, along with three main phases of seafloor spreading, two major plate reorganizations from the late Jurassic to the present. The first phase of spreading started in the northwest–southeast direction and resulted in India's movement away from Antarctic–Australia during the early Cretaceous. During the middle Cretaceous, it appears that the Indian plate rotated from its early NW–SE to N–S direction and moved at a slow spreading rate. During the second phase of spreading, India drifted in the north–south direction from Antarctica with a rapid speed of 11 to 7 cm/yr. The Indian and Australian plates merged and formed a single Indo-Australian plate during the middle Eocene. The third phase of spreading was initiated in the northeast–southwest direction, and appears to continue since then. Also, ridge jumps occur as tectonic events and create more complexity to the evolution of ocean floor, besides plate reorganizations. Due to the processes of ridge jumps and frequent readjustment of the ridge segments, the northern part of the present-day CIR came into existence since the past 30 Ma.

The CIR complex has not been sufficiently explored using satellite geoid/gravity data. Satellite altimetry has recently emerged as an efficient alternative for expensive and hazardous ship-borne gravity surveys[2,3]. The averaged sea surface height as obtained from satellite altimeter is a good approximation to the classical geoid, which contains

*For correspondence. (e-mail: tjmajumdar@sac.isro.gov.in)